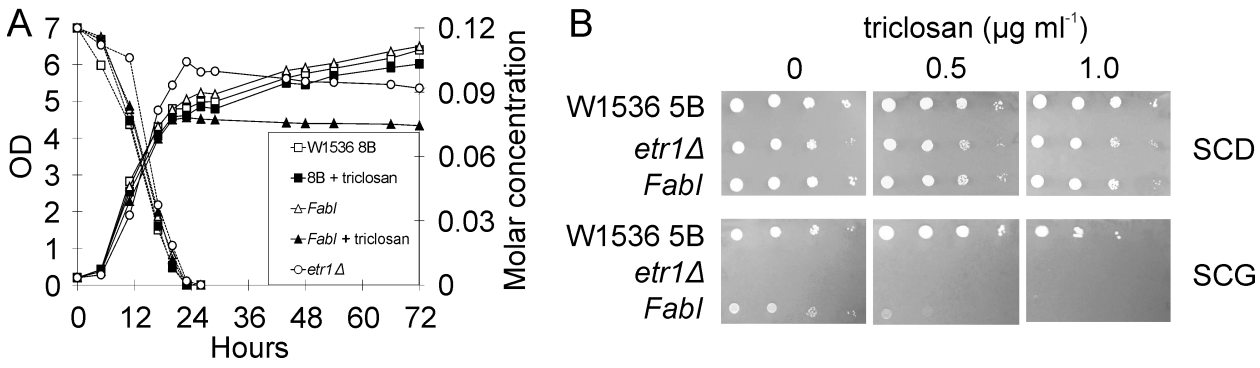

Fig. S1. Characterization of the *FabI* strain. (A) Growth curves of W1536 8B and derivatives. The optical density (OD) values at 600 nanometers are presented as solid lines and molar glucose concentrations as dotted lines. A typical result is shown (B) Dilution series of W1536 5B and derivatives were spotted on solid respiratory glycerol-containing SCG media and fermentable glucose-containing SCD media.

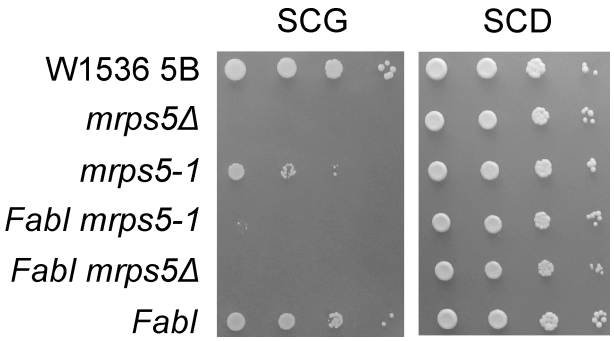

Fig. S2. Example of synthetic petite growth phenotype. The growth characteristics of *mrps5Δ* and *FabI mrps5*Δ + YCp111*MRPS5* (W1536 5B and *FabI*), YCp*lac*111 (*mrps5Δ* and *FabI mrps5Δ*) or YCp111*mrps5-1* (*mrps5-1* and *FabI mrps5-1*) were compared were compared on solid respiratory glycerol-containing SCG and fermentable glucose-containing SCD media.

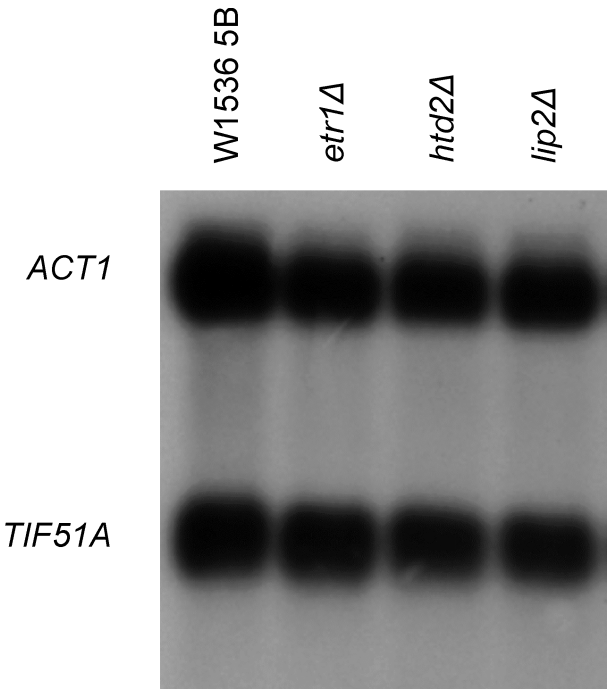

Fig. S3. mRNAs levels of heme-regulated *ANB1/TIF51A* in wild-type, mtFAS and lipoylation defective strains. mRNA levels were estimated by Northern blot analysis as described (Kastaniotis *et al.*, 2000). Actin was used as a loading control. No heme-repressed *ANB1* mRNA, which is slightly shorter than the *TIF51A* message and is visible under de-repressing conditions just below the *TIF51A* band, could be detected in any of the mtFAS defective or lipoylation deficient strains even after prolonged exposure or increased loading. The figure is representative of three independent experiments.

Table S1. Genes identified by mutations that exacerbate a partial mitochondrial fatty acid synthesis pathway deficiency.

Gene	Systematic name	Mutation	Function
Mitochondrial fatty acid synthesis pathway			
CEM1	*YER061c*	G503A → G168D	Mitochondrial β-ketoacyl synthase
		G1094A → G365D*2	
		G1258A → A420T	
HFA1	*YMR207c*	C-273T →Q-91STOP	Mitochondrial acetyl-coenzyme A carboxylase
		G560A → G187D	
		G5459A →1820STOP	
		G5600A → G1867E	
		G5753A → G1918E	
HTD2	*YHR067w*	G3T → M1I	Mitochondrial 3-hydroxyacyl-thioester dehydratase
Post-transcriptional gene expression			
MEF1	*YLR069c*	G1192A → G398R	Mitochondrial translation elongation factor
MRPL16	*YBL038w*	G197A → G66E	Mitochondrial ribosomal protein, large subunit
MRPS5	*YBR251w*	G545A → G182E	Mitochondrial ribosomal protein, small subunit
MSS116	*YDR194c*	G1355A → G452D	Mitochondrial splicing system
RSM22	*YKL155c*	A1559G → E520G	Mitochondrial ribosomal protein, small subunit
Lipoic acid metabolism			
KGD1	*YIL125w*	G2212A → E738K	Mitochondrial α-ketoglutarate dehydrogenase
LIP3	*YJL046w*	G873A →W291STOP	Mitochondrial lipoate-protein ligase
Pyruvate dehydrogenase complex bypass			
ALD4	*YOR374w*	G572T → W191L	Mitochondrial aldehyde dehydrogenase
Transcription factors			
ASK10	*YGR097w*	G3139A → G1047S	Transcription factor, oxidative stress response

Table S2. The statistics of the synthetic petite screen.

Phase of the screen	W1536 5B (**a**) *FabI*	W1536 8B (α) *FabI*	Total	Survivors (%)
Colonies (control)	32 840	27 700	60 540	100
Colonies after mutagenesis	11 440	9 500	20 940	35
Red colonies	111	52	163	0.27
Candidates	65	33	98	0.16
Growth deficiency on SCG	41	30	71	0.12
YCp22*ETR1* complemented	27	12	39	0.06
YEp*FAM1-1* suppressed	5	1	6	0.01

Table S3. Cytochrome *c* oxidase (COX), NADH cytochrome *c* reductase (NCCR), succinate cytochrome *c* reductase (SCCR), and ATPase activity in mitochondrial extracts*.

Strain	COX	NCCR	SCCR	ATPase**
W1536 5B	3.4 ± 0.1 (n = 3)	2.9 ± 0.03 (n = 3)	7.0 ± 0.9 (n = 4)	1.1 ± 0.1 (n = 3)
lip2Δ	2.6 ± 0.2 (n = 3)	2.8 ± 0.2 (n = 3)	2.7 ± 0.5 (n = 4)	1.1 ± 0.04 (n = 3)
lip3Δ	1.3 ± 0.3 (n = 3)	1.6 ± 0.5 (n = 3)	1.8 ± 0.4 (n = 3)	1.1 ± 0.03 (n = 3)
gcv3Δ	1.7 ± 0.2 (n = 3)	1.6 ± 0.1 (n = 3)	2.9 ± 0.1 (n = 6)	1.1 ± 0.04 (n = 3)
etr1Δ	0.6 ± 0.2 (n = 3)	1.5 ± 0.1 (n = 3)	2.8 ± 0.3 (n = 3)	0.67 ± 0.07 (n = 3)

* COX activity is expressed as nanomoles of substrate oxidized per min × mg^{-1} of mitochondrial proteins, NCCR and SCCR activities are expressed as nanomoles of substrate reduced per min × mg^{-1} of mitochondrial proteins and ATPase activity is expressed as micromoles of phosphorus released per min × mg^{-1} of mitochondrial proteins. Data are represented as the mean of at least three measurements ± SD.

**ATPase activity of *etr1Δ* was measured against different W1536 5B wild-type controls. This has been taken into account in Figure 2.

Table S4. Cytochrome *c* oxidase (COX) activity in mitochondrial extracts*.

Strain	COX
iW303-1A	3.3 ± 0.1 (n = 3)
ietr1Δ	0.4 ± 0.1 (n = 3)
ietr1Δ + *mss51*$_{F199I}$	3.3 ± 0.3 (n = 3)
ietr1Δ + *MSS51*	1.5 ± 0.1 (n = 3)

* COX activity is expressed as nanomoles of substrate oxidized per min × mg^{-1} of mitochondrial proteins. Data are represented as the mean of at least three measurements ± SD.

Table S5. Antisense probes for northern blotting.

Name	Sequence	Reference
COX1	5`-TCACCACCTCCTGATACTTCAAA-3`	(Stribinskis *et al.*, 2001)
COX2	5`-GATACTAAACCTAAAATAACTAAT-3`	(Stribinskis *et al.*, 2001)
CYTB	5`-CCTCTTACTACACTTCTATCAGTAAATGG-3`	This study
RPM1	5`-ACTTTTTATTAATATATATATATGGACTCCTGCGGGG-3`	(Schonauer *et al.*, 2008)
SCR1	5`-GTCTAGCCGCGAGGAAGG-3`	(Schonauer *et al.*, 2008)

Additional Results

The growth of the *FabI* strains was indistinguishable from wild-type strains on glucose (Fig. S1A). When *FabI* strains were grown in SCD medium supplemented with triclosan, they grew as well as the wild-type up to the diauxic shift, at which point the growth ceased. While the *etr1Δ* strain and the *FabI* strain supplemented with triclosan ceased growth at approximately the same time point (24 hours), the deletion strain overtook the *FabI* strain after 20 hours and stopped growing at a higher OD (~ 6.0 in *etr1Δ* compared to ~ 4.5 in *FabI*). The higher OD value of the *etr1Δ* strain could be explained possibly by different light scattering of the cells (Torkko *et al.*, 2001) as the wet weight of the cells were less than in the case of wild-type or *FabI*.

The *FabI* strain is indistinguishable from wild-type on glucose (Fig. S1B), but grows slower on glycerol and is inhibited by triclosan under respiratory conditions in a concentration-dependent manner (lower panels).

No heme-repressed *ANB1* mRNA could be detected in any of the mtFAS defective or lipoylation deficient strains (Fig. S3), which is consistent with only a very mild heme deficiency sensed by the cells. It was previously shown that even a seven fold de-repression as measured by the *ANB1-lacZ* reporter barely can be detected by northern blotting (Kastaniotis *et al.*, 2000).

References

Kastaniotis A.J., Mennella T.A., Konrad C., Torres A.M., and Zitomer R.S. (2000) Roles of transcription factor Mot3 and chromatin in repression of the hypoxic gene ANB1 in yeast. *Mol Cell Biol* **20:** 7088-7098.

Schonauer M.S., Kastaniotis A.J., Hiltunen J.K., and Dieckmann C.L. (2008) Intersection of RNA processing and the type II fatty acid synthesis pathway in yeast mitochondria. *Mol Cell Biol* **28:** 6646-6657.

Stribinskis V., Gao G.J., Ellis S.R., and Martin N.C. (2001) Rpm2, the protein subunit of mitochondrial RNase P in saccharomyces cerevisiae, also has a role in the translation of mitochondrially encoded subunits of cytochrome c oxidase. *Genetics* **158:** 573-585.

Torkko J.M., Koivuranta K.T., Miinalainen I.J., Yagi A.I., Schmitz W., Kastaniotis A.J.*, et al.* (2001) Candida tropicalis Etr1p and saccharomyces cerevisiae Ybr026p (Mrf1'p), 2-enoyl thioester reductases essential for mitochondrial respiratory competence. *Mol Cell Biol* **21:** 6243-6253.